

Improvement of the electrochemical properties of Ni-Zn rechargeable batteries by adding B(Pb)SrCaCuO conducting ceramics

G. Ivanova¹, A. Stoyanova-Ivanova², D. Kovacheva³, A. Stoyanova^{1*}

¹ Institute of Electrochemistry and Energy Systems, Bulgarian Academy of Sciences, Acad. G. Bonchev Str, 10, 1113 Sofia, Bulgaria.

² Georgi Nadjakov Institute of Solid State Physics, Bulgarian Academy of Sciences, 72, Tzarigradsko Chaussee Blvd., 1784 Sofia, Bulgaria

³ Institute of General and Inorganic Chemistry, Bulgarian Academy of Sciences, Acad. G. Bonchev Str. 11, 1113, Sofia, Bulgaria

Received November 22, 2018; Revised December 12, 2018

The improvement of the electrochemical properties of Zn-electrode in the Ni-Zn battery cell by adding two types of B(Pb)SrCaCuO conducting ceramics ((Bi_{1.7}Pb_{0.3}Sr₂CuO_x (B(Pb)SCCO 2201) and Bi_{1.7}Pb_{0.3}Sr₂CaCu₂O_x (B(Pb)SCO 2212)) is confirmed. Their presence in the zinc electrode mass increases the discharge capacity of the battery, forming a strong conducting network between the zinc oxide particles. No significant difference in their effect is observed. The shorter thermal treatment synthesis mode of the system (B(Pb)SCCO 2201 must also be taken into account, which determines it to be a more suitable additive in the battery cells under consideration.

Keywords: B(Pb)SrCaCuO conducting ceramics, Zn-electrode, Ni-Zn rechargeable batteries, electrochemical properties

INTRODUCTION

Enhanced interest in rechargeable alkaline nickel-zinc (Ni-Zn) batteries is driven by the wide range of practical applications. These types of batteries possess high energy density (55 – 85 Wh kg⁻¹), high power density (140 -200 W kg⁻¹), high voltage (1,73 V), ability to operate at high current densities, low cost of materials used and low content of potentially environment polluting substances. They do not contain any heavy metals (Hg, Pb, Cd), or flammable active materials and electrolytes and offer a simple recycling process of the metal recovering. Besides, the electrochemical Ni-Zn system is similar as battery technology to the Ni-Cd system widely used in the practice but it is advantageously environmentally friendly by replacing the toxic cadmium with common zinc [1-4]. Nickel-zinc batteries are the ideal choices when there is a need for a small, lightweight power source at a cost significantly lower than that of lithium-ion battery [1,4,5].

Along with the listed advantages, the main disadvantage of this type of rechargeable batteries is the rather poor electrical conductivity of the ZnO electrode, and the limited lifetime expressed in cycles, which is mainly due to the zinc electrode transformation during cycling. The reason for this is the solubility of zinc in the alkaline electrolyte,

leading to the formation of dendrites in the cycling process, accompanied by the formation of short-circuits, which leads to shorter battery lifetime [6,7].

One way to ensure a longer battery lifetime is to add different carbon materials as conductive agents (graphite, carbon foam, acetylene carbon black) into the active mass of the Zn electrode [8]. This, however, induces strong hydrogen evolution during the charging process, which decreases the charge/discharge effectiveness, as well it as may cause mechanical destruction of the electrode mass and reduces the battery life [7].

In order to avoid this disadvantage the application of different conductive oxides and hydroxides as additives to the anode mass attracts the attention of researchers [9]. It is found out that the additions of Ca(OH)₂ and Ba(OH)₂ lead to increasing the battery capacity [9]. Ca(OH)₂ reacts with ZnO to form Ca(OH)₂·2Zn(OH)₂·2H₂O and the resulting complex compound has a low solubility in the electrolyte, which hinders the dissolution of zinc and the formation of dendrites and thus extends the battery lifetime [10,11]. The use of Ba(OH)₂ as an additive to the active mass of the zinc electrode leads to an increase in both the discharge capacity and the cyclability of the electrode. The comparison of the electrochemical behavior of commercial ZnO and zinc oxide doped with Ba(OH)₂ revealed that the capacity of the pure

* To whom all correspondence should be sent:
E-mail: antonia.stoyanova@iees.bas.bg

zinc electrode decreased very steeply compared to that with Ba(OH)₂ additive. In the latter case, mixed barium-zinc hydroxide (BaZn(OH)₄·xH₂O) is obtained, which has an effect analogous to that mentioned above with Ca(OH)₂ additive [12].

In order to improve the properties of the nickel-zinc battery and to study the effects of the additives on the performance of zinc electrode, three content levels of four additives (acetylene black, Bi₂O₃, PbO, Ca [Zn(OH)₃]₂·2H₂O coated by La(OH)₃) that affect the zinc electrode performance were tested with orthogonal design experiments. The experimental evidences indicate that the optimal ratio of electrode additive is as follows: 0.02 g acetylene black, 0.5 g Bi₂O₃, 0.3 g PbO and 0.2 g Ca[Zn(OH)₃]₂·2H₂O coated with La(OH)₃ in a 5 g sample [13].

A modern approach to remove the mentioned disadvantages of the zinc electrode is the use of conductive ceramic powders that not only improve the battery lifetime but they also increase its performance.

Ceramics obtained from various oxides (ZnO)_{0.92} (Bi₂O₃)_{0.054} (ZnO)_{0.92} (Bi₂O₃)_{0.054} (Co₂O₃)_{0.025} (Nb₂O₅)_{0.00075} (Y₂O₃)_{0.00025} were tested as additives to the Zn electrode. It has been found out that Zn electrode with addition of conductive ceramic demonstrates improved electrochemical properties, such as higher discharge capacity, cycling stability and efficiency compared to the zinc electrode with pure nanosized ZnO. The observed positive effect is explained by the formation of a highly conductive network of metals Bi, Co and Y during cycling, which helps to improve the electrical contact between ZnO particles and increases their active surface area [14,15].

The high-temperature superconductors are discovered in 1986 by Georg Bednorz and K. Alex Müller [16] and since then the technological research has been focused on producing high-temperature superconductor (HTS) materials in sufficient quantities to optimize their properties in relation to a wide range of advanced applications. The superconductors of the cuprate ceramic systems Y-Ba-Cu-O (YBCO) [17,18] are a representative of the most advanced HTS materials with potential large-scale engineering applications. Their chemical stability is one of the most important factors for their practical application. In our previous paper the possibility of using YBCO and BSCCO [19,20] powders of superconducting materials as additives to the zinc electrode mass of nickel-zinc alkaline rechargeable batteries was studied. The high chemical resistance of the ceramics to the battery electrolyte has been confirmed by structural and surface morphology

observations, as well as by magnetic measurements of ceramic samples after prolonged exposure to the alkaline electrolyte. The electrochemical tests have shown that the zinc electrode with YBCO ceramic additive (7 wt.%) exhibits good cycling ability and capacity stability, and higher (by 30%) specific discharge capacity than the zinc electrode with a "classic" conductive carbon additive [21,22].

The results of the electrochemical studies show that the nickel-zinc battery cell with zinc electrode with active mass containing superconducting BSCCO (2212) and BSCO (2201) ceramic additive also exhibits good cycling ability and performance stability during prolonged charge-discharge cycling. The measurements of the electric resistance of the composite electrode masses have shown that the resistance of the zinc electrode mass with addition of Bi_{1.7}Pb_{0.3}Sr₂Ca₂Cu₃O_x ceramic (230 ohm.cm) is by about 30% lower than the resistance of the electrode mass with carbon additive (330 ohm.cm). It is supposed that the superconducting powder forms a highly conductive network between the particles of the zinc oxide in the electrode mass, thus improving the electric contact in the power generation material of the zinc electrode. The addition of BSCCO ceramics improves not only the conductivity and electrochemical homogeneity of the electrode mass and reduces the gas evolution (because of the absence of carbon materials with a low-overpotential of hydrogen evolution) but it also stabilizes its porosity structure [23-25].

The aim the present paper was to compare two types of cuprate ceramics (B(Pb)SCO 2212 and B(Pb)SCCO 2201) as additives to the zinc electrode mass in the rechargeable alkaline Ni-Zn batteries. For this purpose, they are structurally characterized and subjected to charge-discharge electrochemical cycling tests in alkaline electrolyte according to preliminary-developed test methodology. The possible mechanism of their action is discussed.

EXPERIMENTAL

Synthesis of B(Pb)SCO 2212 and B(Pb)SCCO 2201

Powder samples of two modifications Bi_{1.7}Pb_{0.3}Sr₂CaCu₂O_x (B(Pb)SCO 2212) and Bi_{1.7}Pb_{0.3}Sr₂CuO_x (B(Pb)SCCO 2201) were prepared by the standard solid state reaction from high-purity oxides of Bi₂O₃, PbO, CuO, SrCO₃ and CaCO₃. After mixing, grinding and initial heat treatment at 780°C for 24 hours in air atmosphere the powder obtained was ground and pressed into pellets (5-6 MPa). In air atmosphere the B(Pb)SCCO 2201 was sintered at 830°C for 24 hours and B(Pb)SCO 2212 at 830°C for 48 hours.

The pellets of sintered ceramic samples (10 mm diameter, 2 mm thick) were first soaked in 50 ml of 7M solution of KOH and then exposed to the alkaline solution for 24, 48, 72 or 96 hours. Then they were removed from the solution and dried at room temperature. Since the changes of all samples towards the exposure period (time) were practically negligible, further in the paper only results for the longest soaking time (96 hours) are presented.

Preparation of the zinc electrode and battery assembling

Preparation of the zinc paste. The electrochemically active nanosized powdered ZnO was produced by a solution combustion method using as initial compound $Zn(NO_3)_2 \cdot 6H_2O$ and sucrose. The amorphous powder oxide material produced after evaporation of the water was subjected to thermal treatment at 600 °C in order to obtain the appropriate size of the crystallites.

The electrode mass is composed of powdered ZnO (88 wt.%), conducting additives – cuprate ceramic powder B(Pb)SCO 2212 and B(Pb)SCCO 2201, and carbon (acetylene black) (7 wt.%) and binding agents – polytetrafluorethylene (PTFE, 4 wt.%) and carboxymethylcellulose (CMC, 1 wt.%). The electrode mass was thoroughly mixed with a certain amount of distilled water to form mushy paste according to a procedure developed previously and described in detail [26,27].

Pasted electrode and battery assembling. Zinc electrode prepared by inserting the zinc paste into the matrix of copper foam (successively covered with tin and zinc) with dimensions 5.0×3.0 cm (thickness 0.15 cm) was used as current collector and carrier of the zinc mass. The pasted electrode was dried at 70°C for 2 hours, pressed under 30 MPa for 2 min and then mounted into a separator pocket made of a polypropylene type of microporous separator (Celgard C3501, Celgard, USA). A solution of 7M KOH was used as a battery electrolyte. The electrode-separator package was soaked under vacuum with battery electrolyte for 10 min before mounting it in the prismatic nickel-zinc battery cell. Sintered type of nickel electrodes (CLAIO, Poznan, Poland) with dimensions 5.0×3.0 cm and thickness 0.12 cm, and a nominal capacity about two times higher than that of the zinc electrodes, were used for cathodes in the nickel-zinc battery cell. The electrodes were directly wetted with the electrolyte before mounting in the cell using the same evacuation procedure. The container of the prismatic battery cell was made of a transparent plastic material and the cell was assembled with two nickel cathodes and one zinc anode [27].

Physicochemical and electrochemical characterization. The X-ray diffraction patterns of the ceramic powdered samples were obtained within the range of 5.3 to $80^\circ 2\theta$ at a constant step of $0.02^\circ 2\theta$ on a Bruker D8 Advance diffractometer with $Cu K\alpha$ radiation and a LynxEye detector. The phase identification was performed by a Diffrac plus EVA v. 15 program using the ICDD-PDF2 data base. The mean crystallite size and the unit cell parameters were determined by the Topas v.4.2 software package using the fundamental parameters peak shape description including appropriate corrections for the instrumental line broadening and diffractometer geometry [28].

The electrochemical investigations of the nickel-zinc battery cells were carried out under galvanostatic conditions using an automatic battery testing apparatus CDT10. The apparatus gives a possibility for complex control and monitoring of the main cell parameters during charge/discharge cycling - cell voltage and current, capacity and temperature. The zinc electrodes were characterized by the developed test methodology comprising the several steps already described in [29].

The efficiency of the electrodes was determined by the equation:

$$\eta = Q_{\text{disch}} / Q_{\text{ch}} \cdot 100\% \quad (1),$$

where Q_{disch} is the discharge capacity, and Q_{ch} - the charge capacity of the electrode.

RESULTS AND DISCUSSION

Our previous investigations show that no phase changes in the semiconducting B(Pb)SrCaCuO ceramics have occurred after prolonged contact of the samples with a strong alkaline solution (7 M KOH). After treatment in the alkaline solution no essential changes in the bulk morphology of the BSCCO samples were observed too [23].

X-ray diffraction patterns of the cuprate ceramics B(Pb)SCCO 2201 and B(Pb)SCO 2212 are given in Figures 1 and 2, respectively.

Based on XRD analysis a single phase in a well crystallized form of both investigated ceramics is observed. Secondary phases are not detected.

The refined unit cell parameters for B(Pb)SCCO 2201 are $a = 5.3920 \text{ \AA}$; $b = 24.6030 \text{ \AA}$; $c = 5.3000 \text{ \AA}$ with orthorhombic unit cell volume $V_m(\text{B(Pb)SCCO 2201}) = 703.09 \text{ \AA}^3$ (Fig.1a) and those for B(Pb)SCO 2212 are $a = b = 5.395 \text{ \AA}$; $c = 30.714 \text{ \AA}$, with tetragonal unit cell volume $V_m(\text{B(Pb)SCO 2212}) = 893.962 \text{ \AA}^3$ (Fig. 1b).

It is noticeable that the structure of the obtained ceramics differs from that of the ceramic additives used so far [14, 15]. Under certain conditions these

ceramics can exhibit superconducting properties [16-18].

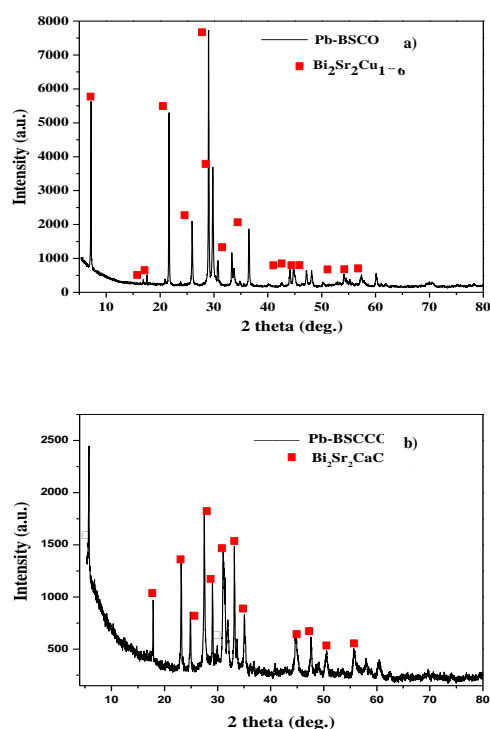


Figure 1. Powder X-ray diffraction pattern of B(Pb)SCCO 2201 (a) and B(Pb)SCO 2212 (b) ceramics.

The electrochemical tests of the zinc electrodes with additives of B(Pb)SCCO 2201 and B(Pb)SCO 2212 ceramics were conducted according to the developed methodology, which includes several charge/discharge current modes up to the critical maximum 9C [29]. For comparison, the same tests were carried out with conventional carbon additive (acetylene black). In Figs. 2 and 3 the voltage-time curves are shown (the 8th cycle) of the zinc electrode with B(Pb)SCCO 2201, B(Pb)SCO 2212 and carbon conductive additives at 1C and 9C, respectively.

As it is seen in Fig. 2, the electrochemical processes under this current mode proceed without the occurrence of any side effects. The main difference in the voltage profiles is the higher value of perceived charge at DC current in the cells with BSCCO additive compared to that of a cell with a carbon additive. This can be explained with the better conductivity of the cuprate ceramics used over that of carbon.

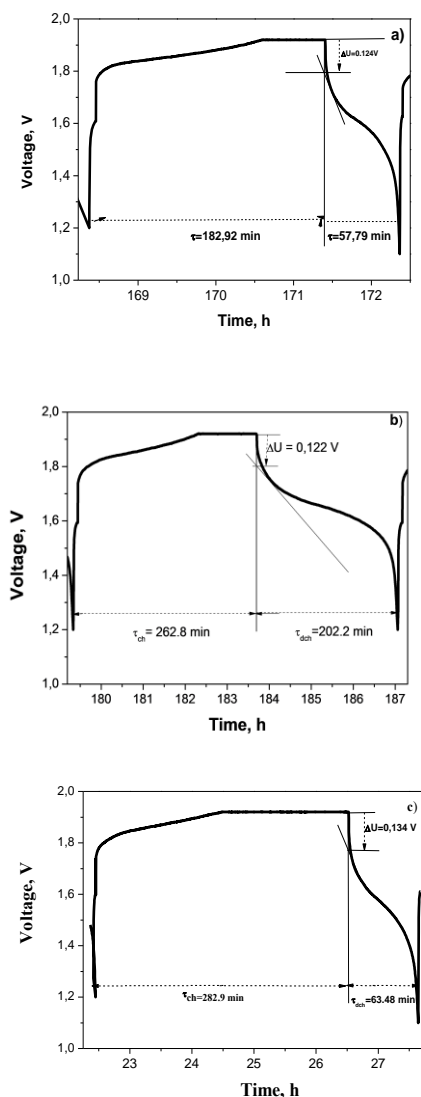


Figure 2. Charge/discharge curves of the Ni/Zn cells with B(Pb)SCCO 2201 (a), B(Pb)SCO 2212 (b) and carbon (c) additives to the active mass of the zinc electrode at current loads 30 mA g^{-1} (mode 1C).

The data in Table 1 show that the initial voltage drop at the beginning of the discharge process is lower for Zn electrodes with ceramic additives ($\Delta U_{B(Pb)SCCO\ 2201} = 0,124V$, $\Delta U_{B(Pb)SCO\ 2212} = 0.122V$, $\Delta U_c = 0.134V$), respectively their lower resistance is ($R_{B(Pb)SCCO\ 2201} = 4.13$, $R_{B(Pb)SCO\ 2212} = 4,27$, $R_c = 4.47$). No significant difference is observed comparing both electrodes with B(Pb)SrCaCuO additive.

Another important advantage of the ceramics-modified zinc electrodes is the higher efficiency of their operation (93.80% and 96.82%, respectively), which exceeds by 16-18% that of the carbon-doped electrode (78.90%). The role of the additive is reflected in its contribution to reducing hydrogen releases during the charging of the electrode.

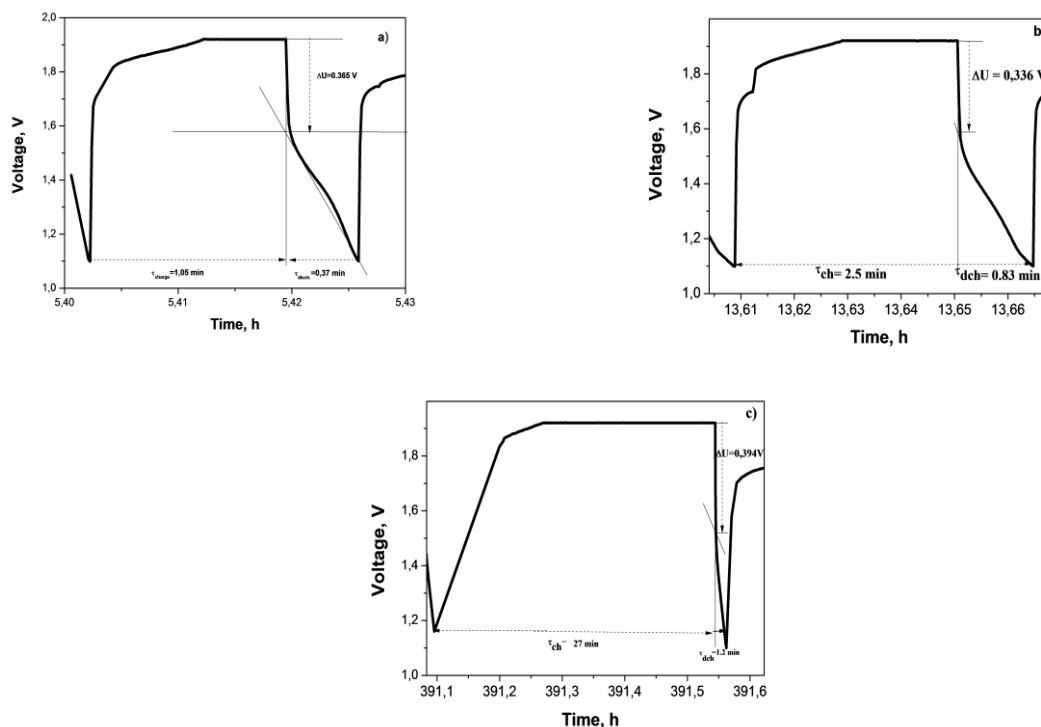


Figure 3. Charge/discharge curves of the Ni/Zn cells with B(Pb)SCCO 2201 (a), B(Pb)SCO 2212 (b) and carbon (c) to the active mass of the zinc electrode at current loads of 270 mA g⁻¹ (mode 9C)

Table 1. Calculated values based on charge/discharge curves for Zn electrodes with different additives (current mode 1C and 9C): ΔU- voltage drop, Q_{ch}/Q_{disch} - charge/discharge capacitance, Θ – efficiency

Additive	ΔU, V		Q _{ch} , mAh		Q _{disch} , mAh		Θ, %	
	1C	9C	1C	9C	1C	9C	1C	9C
B(Pb)SCCO 2201	0.124	0.365	1.662	0.223	1.562	0.213	93.80	95.52
B(Pb)SCO 2212	0.122	0.336	1.386	0.288	1.342	0.260	96.82	90.27
Carbon	0.134	0.394	1.341	0.226	1.058	0.180	78.90	79.60

The voltage-time curves of Ni/Zn cells with B(Pb)SrCaCuO and carbon modified electrodes performed at extreme current mode (9C, 270 mA g⁻¹) are shown in Fig. 3.

Fig. 3 shows that the voltage profile does not change significantly and even under these extreme conditions the B(Pb)SrCaCuO-modified conductive ceramic electrodes perceive more than 50% of the DC charge. The initial voltage drop is low ($\Delta U_{B(Pb)SCCO\ 2201} = 0.365\text{ V}$, $\Delta U_{B(Pb)SCO\ 2212} = 0.336\text{ V}$), and in this case the voltage profile has a plateau character at a high average voltage of 1.615 V. The efficiency of these electrodes is also high (90 - 95%).

The Zn electrode with carbon additive is strongly polarized ($\Delta U_C = 0.394\text{ V}$) and it shows significantly lower average discharge voltage (1.409 V) and much lower capacitive values and efficiency (79.60%), compared to the ceramic-modified electrodes. The dependences of the specific capacity for the electrodes on the number

of charge-discharge cycles during prolonged cycling are shown in Figure 4.

Comparing the capacity of the cells with zinc electrodes containing carbon and ceramic additives show that the presence of two modifications B(Pb)SCCO 2201 and B(Pb)SCO 2212 of a ceramic additive to the negative active mass of a Ni-Zn battery results in higher and more stable specific discharge capacity in comparison to the zinc electrode with classic carbon additive, especially under high current (0.5 A) [25, 26, 29]. At the beginning the discharge capacity of the carbon-containing electrode exceeds by about 11% that of the electrodes with B(Pb)SrCaCuO ceramics, but this electrode is unstable and it drops steeply with the increase in the cycle numbers. The discharge capacity of the cells with B(Pb)SrCaCuO conductive additives is by more than 30% higher than that of the conventional zinc electrode and is stable over 500 cycles. This result can be explained by the formation of a highly conducting network between the zinc oxide particles in the electrode mass in the presence of cuprate ceramics.

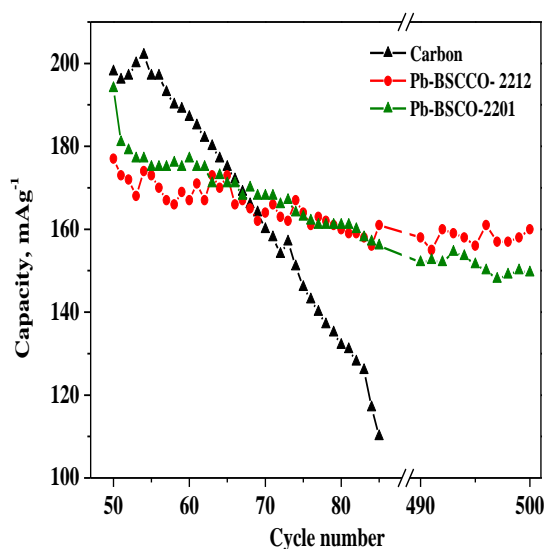


Figure 4. Dependence of the specific discharge capacity of the zinc electrode with carbon, B(Pb)SCCO 2201 (a) and B(Pb)SCO 2212 (b) ceramic additives on the cycle number, at current load C/5 (0.2 A)

CONCLUSION

The electrochemical characteristics of the Ni-Zn battery cell were enhanced by adding two types of Bi(Pb)SrCaCuO conducting ceramics ($\text{Bi}_{1.7}\text{Pb}_{0.3}\text{Sr}_2\text{CuO}_x$ (B(Pb)SCCO 2201) and $\text{Bi}_{1.7}\text{Pb}_{0.3}\text{Sr}_2\text{CaCu}_2\text{O}_x$ (B(Pb)SCO 2212)) to the zinc electrode mass. The conducted electrochemical tests confirmed the positive effect of both ceramics on the battery electrochemical properties at prolonged cycling, as no substantial difference in their effect was established. The results obtained can be explained again by an increase in the conductivity and homogeneity of the electrode mass in the presence of the additives used, on the one hand, and the formation of a highly conducting network between the zinc oxide particles, on the other. The shorter thermal treatment synthesis mode of B(Pb)SCCO 2201 ceramic determines it to be a more suitable additive in the battery cells under consideration.

Acknowledgements: The experiments were performed with equipment included in the National Infrastructure NI SEVE supported by the Ministry of Education and Science under grant agreement № DOI-160/28.08.18.

The authors express their sincere thanks to Prof. R. Raicheff, Assoc. Prof. Ml. Mladenov and Eng. Lozan Stoyanov for their invaluable help in the preparation of this work.

REFERENCES

1 M. Geng, D. Northwood, *Int. J. Hydrogen. Energ.*, **28**, 633 (2003).

2 H. Mcgraw (ed.) Handbook of batteries (New York, 2004).

3 S. Philips, S. Mohanta, M. Geng, J. Bartom, Mc Kinney, J.Wu, *ECS Trans.*, **16**, 11 (2009).

4 G. Zhang, *ECS Trans.*, **16**, 47 (2009).

5 R. Raicheff, M. Mladenov, L. Stoyanov, N. Boshkov, V. Bachvarov, *Bulg. Chem. Commun.*, **48**, 61 (2016).

6 M. Ma, J. Tu, Y. Yuan, X. Wang, K. Li, F. Mao, Z. Zeng, *J. Power Sources*, **179**, 395 (2008).

7 W. Long, Z. Yang, X. Fan, B. Yang, Z. Zhao, J. Jing, *Electrochim. Acta*, **12**, 40 (2013).

8 H. Tao, X. Tong, X. Gan, S. Zhang, X. Liu, *J. Alloys Compd.*, **658**, 119 (2016).

9 Y. Zheng, J. Wang, H. Chen, J. Zhang, C. Cao, *Mater. Chem. Phys.*, **84**, 99 (2004).

10 Y. Yuan, J. Tu, H. Wu, Z. Zhang, X. Huang, X. Zhao, *Electrochem. Commun.*, **8**, 653 (2006).

11 R. Shivkumar, S. Umamaheswari, G. Kalaignan, T. Vasudevan, *Indian J. Chem.Technol.*, **8**, 95 (2001).

12 J. Wang, C. Zhang, L. Zhang, J. Zhang, C. Cao, *Mater. Chem. Phys.*, **70**, 254 (2001).

13 G. Cheng, Y. Zhang, W. Zhao, W. Yu, H. Hou, *Met. Soc. China*, **2**, 3551 (2014).

14 H. Huang, L. Zhang, W. Zhang, Y. Gan, G. Shao, *J. Power Sources*, **184**, 663 (2008).

15 L. Zhang, H. Huang, W. Zhang, Y. Gan, C.Wang, *Electrochim. Acta*, **53**, 5386 (2008).

16 J. Bednorz, K. Müller, *Z. Phys. B.*, **64**, 189 (1986).

17 M. Wu, J. Ashburn, C. Torng, P. Hor, R. Meng, L. Gao, Z. Huang, Y. Wang, C. Chu, *Phys. Rev. Lett.*, **58**, 908 (1987).

18 V. Kovachev, E. Vlachov, K. Nenkov, V. Lovchinov, M. Gospodinov, A. Stoyanova, D. Dimitrov, M. Czyczek, *Intern. J. Modern Phys. B*, **1**, 479 (1987).

19 C. Michel, M. Hervieu, M. Borel, A. Grandin, F. Deslandes, J. Provost, B. Raveau, *Phys. B-Condensed. Matter.*, **68**, 421 (1987).

20 H. Maeda, Y. Tanaka, M. Fukotomi, T. Asano, *Jpn. J. Appl. Phys. Lett.*, **27**, 209 (1988).

21 G. Ivanova, A. Stoyanova-Ivanova, S. Terzieva, D. Kovacheva, M. Mladenov, B. Blagoev, D. Dimitrov, Proceedings of the 12th Cryogenics International Conference, **11** (2012).

22 A. Stoyanova-Ivanova, S. Terzieva, G. Ivanova, M. Mladenov, D. Kovacheva, R. Raicheff, S. Georgieva, B. Blagoev, A. Zaleski, V. Mikli, *Bulg. Chem. Commun.*, **47**, 221 (2014).

23 G. Ivanova, L. Stoyanov, S. Terzieva, A. Stoyanova-Ivanova, M. Mladenov, D. Kovacheva, R. Raicheff, *Nanoscience&Nanotechnology*, **14**, 33 (2014).

24 L. Stoyanov, S. Terzieva, A. Stoyanova, A. Stoyanova-Ivanova, M. Mladenov, D. Kovacheva, R. Raicheff, *JPRC*, **2**, 83 (2016).

25 G. Ivanova, L. Stoyanov, A. Stoyanova, M. Mladenov, R. Raicheff, *Nanoscience & Nanotechnology*, **16**, 27 (2016).

26 M. Mladenov, R. Raicheff, L. Stoyanov, A. Stoyanova-Ivanova, S. Terzieva, D. Kovacheva, *BG Patent Reg. # 111 646* (in Bulgarian) (2013).

- 27 M. Mladenov, R. Raicheff, L. Stoyanov, D. Kovacheva, *BG Patent Reg. # 111 775* (in Bulgarian) (2014).
28 PAS V4: General profile and structure analysis software for powder diffraction data, User's Manual, Bruker AXS, Karlsruhe, Germany, Bruker AXS (2008).
29 G. Mitrova, PhD Thesis (IEES-BAS Bulgaria) (2015).